Microgravity Science and Technology (2022) 34: 26
https://doi.org/10.1007/s12217-022-09945-4

ORIGINAL ARTICLE

Flame Spread over Polyethylene Film: Effects of Gravity and Fuel Inclination

Feng Zhu[1] · Xinyan Huang[2] · Shuangfeng Wang[1,3,4]

Received: 20 January 2022 / Accepted: 29 March 2022 / Published online: 23 April 2022

Abstract

The flammable thermoplastics are widely used in our daily life and manned space travels in microgravity, posing a potential fire risk. This work studies the flame spread along with the thin polyethylene (PE) film (15–100 μm) in the microgravity drop tower and normal gravity. Microgravity flame spread faster than vertically downward flame spread in normal gravity due to the weak buoyancy flow and greater flame preheating length. For the ultra-thin film, the influence of melting on the opposed flame spread is negligible. The upward flame spread rate reaches a maximum constant (45 ± 10 mm/s for 20 μm film) when the inclination angle is larger than 30°, due to the dripping removal of molten fuel. The upward flame spread rate changes under the competition between the enhanced flame heating by buoyancy and the dripping removal of the molten fuel. The vertically upward spreading flame cannot be maintained due to the dripping removal of the molten fuel, and a critical extinction condition was determined and analyzed. This work provides valuable data on flame dynamics in plastic films and can help develop more sophisticated material flammability tests for fire safety in space travel.

Keywords Microgravity combustion · PE · Inclination angle · Flame spread · Extinction

Nomenclature

Symbols

Bi	Biot number (-)
c	Specific heat (kJ/kg/K)
D	Diameter (m)
g	Gravitational acceleration (m/s^2)
h	Convection heat transfer coefficient (W/m^2/K)
l	Length (m)
L	Characteristic length (m)
L_v	Latent heat of vaporization (J/kg)
M	Mass (g)
$\dot{m}$	Mass loss rate (g/s)
Nu	Nusselt number (-)
Pr	Prandtl number (-)
$\dot{q}''$	Heat flux (kW/m^2)
R	Radius (m)
Ra	Rayleigh number
t	Time (s)
T	Temperature (K)
V	Spread rate (m/s

Greeks

α	Thermal diffusivity (m^2/s)
β	Thermal expansion coefficient (K^{-1})
δ	Length (m)
θ	Angle (°)
λ	Heat conductivity (W/m/K)
μ	Viscosity (kg/m/s)
ν	Kinematic viscosity (m^2/s)
ρ	Density (kg/m^3)
σ	Surface tension (N/m)
τ	Thickness (m)

Subscripts

∞	Ambient
b	Burning
cr	Critical

✉ Xinyan Huang
xy.huang@polyu.edu.hk

✉ Shuangfeng Wang
sfwang@imech.ac.cn

[1] Key Laboratory of Microgravity, Institute of Mechanics, Chinese Academy of Sciences, Beijing 100190, China

[2] Research Centre for Fire Safety Engineering, Department of Building and Environmental Engineering, The Hong Kong Polytechnic University, Hong Kong, China

[3] State Key Laboratory of High-Temperature Gas Dynamics, Chinese Academy of Sciences, Beijing 100190, China

[4] School of Engineering Science, University of Chinese Academy of Sciences, Beijing 100049, China

dr	Drip
f	Flame
g	Gas
ig	Ignition
m	Melt
s	Solid
tot	Total

Introduction

Fire safety is an important issue in human-crewed space missions, where a large amount of combustible plastics were inevitably used. However, in case of a fire event, the capacity of firefighting, smoke ventilation, and human evacuation are limited (Ross 2001). Various ground-based fire tests, spacecraft experiments, and numerical simulations have been made to study the fire behaviors of solid fuels in microgravity (Fujita 2015; Rojas-Alva and Jomaas 2022). For example, the microgravity flame spread dynamics and typical fuels, such as cellulose papers (Olson 1991; Olson et al. 1989; Ramachandra et al. 1995; Vetturini et al. 2020; Wang et al. 2015), PMMA (Hu et al. 2014; Link et al. 2018; Olson et al. 2004; Urban et al. 2019; Wang and Zhu 2019; Wu et al. 2020a, b; Zhu et al. 2019), thin wires (Fujita et al. 2002; Nagachi et al. 2019; Takahashi et al. 2013), PDMS membranes (Rojas-Alva et al. 2022) and fabrics (Takahashi et al. 2020, 2019; Zhao et al. 2017), have been investigated and compared with normal-gravity dynamics. In particular, thermoplastic materials, such as polyethylene (PE) and polyurethane (PU), are widely used for electrical wires and insulation materials in human-crewed spacecraft. When the thermoplastic is heated, it will first melt into liquid before ignition (Nagachi et al. 2019; Takahashi et al. 2013). In normal gravity, the thermoplastic melts will flow and drip driven by gravity force, but in microgravity, the surface tension tends to pull the melt into spherical shapes (Takahashi et al. 2013) and burn like a droplet (Migita et al. 2020; Sun et al. 2020). Such phase-change processes of thermoplastics can also change the flame-spread behaviors in microgravity, which are still not well understood.

The thermoplastics can be made into thin film due to their excellent transparency, ductility, and malleability. For example, PE film is widely used for food bags and greenhouse farming in the space environment. Due to the small thermal inertia and a low oxygen index (Tewarson 2003), the PE film can be ignited easily and support flame spread (Ikeda 2018). For a thermally thin solid fuel, the flame spread rate decreases with the increase of the sample thickness (Quintiere 2006). Moreover, a steady flame spread rate can be achieved easily for a thin fuel, when the rate of burnout equals the rate of piloted ignition. With the increase of the opposed flow velocity, three regimes can be identified, (1) the low-velocity Radiation Regime (or oxygen-limited Regime), where flame spread rate increases, (2) the Thermal Regime, where the flame spread rate is independent of the opposed flow, and (3) the Kinetic Regime, where the flame spread rate decreases until extinction (Bhattacharjee et al. 2003; Fernandez-Pello et al. 1981; Olson 1991; Olson et al. 1989). The low-velocity regime and the extinction by limited oxygen (smothering) can be easily observed in microgravity due to the removal of buoyancy flow and the increasing role of the radiative and conductive heat losses (Altenkirch et al. 1998; Bhattacharjee et al. 2005; Link et al. 2018; Olson et al. 2004; West et al. 1996; Wu et al. 2020a, b; Zhu et al. 2019). Three similar regimes can also be observed under the concurrent airflow (Kumar et al. 2003; Loh and Fernandez-Pello 1985; Lu et al. 2019a; Urban et al. 2019). When the fuel thickness further decreases to ultra-thin, the flame spread rate becomes comparable with the airflow velocity, which changes the flame from the concurrent spread to the opposed spread (Vetturini et al. 2020).

For the fire safety of manned spacecraft, solid materials used in the cabin must pass strict ground-based fire safety standard tests to evaluate their flammability properties, such as Test 1 of NASA-STD-6001B (NASA-STD-6001B 2011), which tests the upward flame spread over the target material. Multiple ground-based fuel inclination tests have confirmed that the vertical upward flame spread is the fastest model that can represent the worst fire scenario, such as found in thin plastic sheets (Quintiere 2001) and paper (Comas and Pujol 2013; Quintiere 2001), thin wire (Hu et al. 2015; Lu et al. 2019b), and thick PMMA (Drysdale and Macmillan 1992; Gollner et al. 2013; Ito and Kashiwagi 1988; Zhou et al. 2020). However, it still is a big approximation to use ground-based experiments to guess the material flammability and fire behaviors in microgravity. Especially for thermoplastic materials, the flow and dripping of melts driven by gravity may change the flammability, flame-spread rate (Kobayashi et al. 2020), and extinction limit (Miyamoto et al. 2016). Thus, the conventional ground-based experiments may no longer reflect worse fire scenarios, which can be referred to for the fire safety in microgravity. For example, experiments showed that the ignition delay time of PE was shorter in the microgravity field due to the lack of cooling by natural convection (Ikeda 2018). So far, very limited combustion experiments are available for the thermoplastic polyethylene film.

In this work, we investigate the microgravity flame-spread behaviors on thin PE film (15–100 μm) via the drop tower experiment. The comparative normal-gravity experiments are conducted for flame spread over PE films of different inclinations to identify the scenarios that have the largest fire hazard and are closest to the microgravity. In addition, the effects of melting and dripping of molten PE on flammability and flame spread are discussed.

Experiments

Microgravity Experiments

The microgravity experiments were conducted in the 3.6-s drop tower in the Chinese Academy of Science, which offered a microgravity level of 10^{-3} g for the single-capsule test (Sun et al. 2020; Wang et al. 2015; Wu et al. 2020b). Sample holders used in the experiments were shown in Fig. 1. The HDPE (high-density polyethylene) film sample was 50 mm wide and 80 mm long. The film sample was mounted and flattened on a thin inert mica frame which was 1-mm thick. PE films with four thicknesses of 15, 20, 30, and 40 μm were used in the microgravity experiments. However, for the 40-μm sample, the flame was just formed after the capsule was on ground. For 20-μm sample, the flame spread experiment was repeated to verify the reliability. The thermogravimetric analysis (TGA) analysis of the PE sample can be found in the Appendix and Fig. 11, where its pyrolysis temperature is about 410 °C.

Ignition in these experiments was achieved just prior to the drop in normal gravity using a Ni–Cr heat wire. To achieve a uniform ignition in one end, a 1 cm-long ignition tissue paper strip with an area density of 8 g/m^2 was wrapped by a heating Ni–Cr wire and placed on the top of the PE film (see Fig. 1). The power supply of the ignition wire was 132 W (12 V and 11 A). Ignition in normal gravity generally occurred after heating for about 3 s. After a stable flame was formed and spread away from the hot coil, the capsule was then released. Due to the initial upward buoyancy flow, the observed flame spread was opposed in nature. Note that without gravity and buoyancy flow, the concepts of upward and downward flame spread as well as the fuel orientation in normal gravity become invalid. Inside the drop capsulate, an on-board video camera was placed to capture the flame evolution before and during the drop test from the front view.

To evaluate the influence of the ignition hot wire on the deformation of PE film and the rate of flame spread, additional base experiments were carried. The 20-μm PE film was positioned 2 mm below the hot coil, and the coil igniter had sufficient ignition power and lasted for more than 1 min. Results showed that even with a greater ignition power and duration, the film was not curling, deformed, or pyrolyzed by the hot coil, so the influence of igniter on the flame spread was limited.

Fig. 1 The PE film sample and the sample holder used in the drop tower microgravity experiments

Normal Gravity Experiments

The same PE film sample, test apparatus, and ignition methods were used in the normal-gravity test. In addition, the sample holder was made to be rotatable to test the flame spread under different fuel inclinations, as shown in Fig. 2a and b. A GoPro Hero 7 digital camera with a resolution of 1920 by 1080 at 24 fps was used to record the front view of the burning process. To facilitate the observation and image analysis, all tests were performed in a dark room. In order to observe the dripping moving and burning process, a high-speed camera (AOS TRI-VIT) at 500 fps with a resolution of about 0.1 mm/pixel was used from side. Two mass balances, which were placed up and down respectively, were used to measure the variation of the fuel mass and the dripping mass simultaneously.

PE films with eight thicknesses of 15, 20, 30, 40, 60, 80, 100, and 375 μm were used in normal gravity experiments. The samples were tested over angles ranging from + 90° (vertical upward) to -90° (vertically downward), where $\theta < 0$ represents a downward flame spread, and $\theta > 0$ represents an upward flame spread. Once the fuel sample was ignited, the buoyancy force maintained an upward flame above the PE sample. All the tests were repeated at least three times to reduce random error. As a reference, the flame spread over the tissue paper with a thickness of 45 μm and an area density of 8 g/m^2 were also tested for comparison.

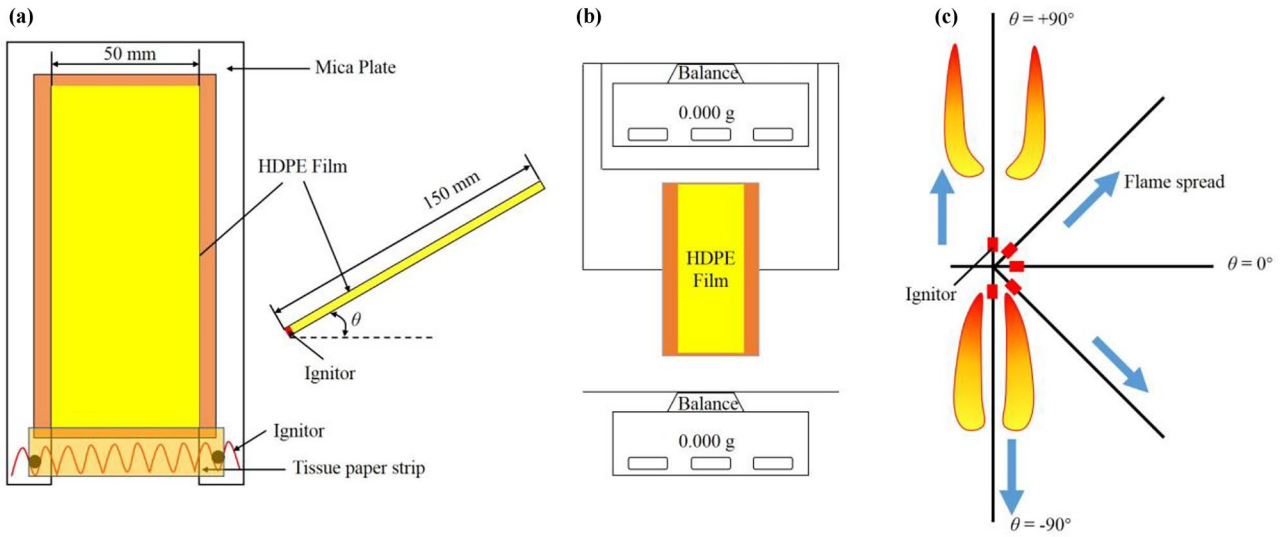

Fig. 2 Illustrations of (**a**) side-view and front-view of the fuel sample, (**b**) experimental set up and (**c**) flame spread configurations and fuel inclinations in normal gravity

Results and Discussion

Microgravity Opposed Flame Spread

Figure 3 shows the flame spreading over PE with a thickness of 15 and 20 µm before and during the microgravity drop period (see Video S1 in the Supplemental Materials). The influence of ignition was minimized because the PE film was ignited, and the flame spread away from the coil ignitor before the drop.

For the 15-µm film (Fig. 3a), a short, weak, and dark red flame was observed right after entering the microgravity environment (see $t = 0$ s). After about 0.2 s, a continuous flame was sustained. Then, the flame front separates into several sub-fronts (flamelets), and some flamelets were extinguished locally. Thus, only a small part of the film was still burning like the fingering phenomena (see $t = 1.8$–3.6 s). During this process, the flame becomes weak, and the film edge was curling towards the direction of flame spread due to the larger surface tension at the relatively cold region (or the Marangoni effect).For the 20-µm film (Fig. 3b), a bright yellow flame, which is caused by the pyrolysis of the PE film, can be observed right after the drop (see Video S2). At about $t = 0$ s, the flame starts to break up. After about 1 s, the original bright and orange-color flame became weak and pale blue, and at about $t = 2$ s, the separation is completed. At about 3 s, the uniform flame gradually extinguishes, and only a small flamelet survives a little longer approaching the lower right corner. Moreover, the PE film was curling in the direction of flame spread, and the whole film edge continues to move and shrink after the flameout. The flame spread behaviors for the 30-µm and 40-µm films are similar to the 20-µm film. In general, for a thinner PE film, the flame leading edge tends to split and partially extinguished in microgravity, while for a thicker PE film, the flame leading edge tends to keep together and continuous.

Downward Flame Spread in Normal Gravity

Figure 4 shows the evolution of vertically downward ($\theta = -90°$) flame spread over a 20-µm PE film in normal gravity (also see Video S3). Similar to the opposed flame spread in microgravity in Fig. 3, the uniform flame first forms and then separates into multiple flamelets, and the local extinction also occurs temporarily during the downward flame spread. Some flame sub-front spreads in the transverse direction locally. Similar flamelets separation and the near-limit fingering flame spread had been observed in thin filter paper previously in both microgravity and normal gravity (Olson et al. 1998; Zhang et al. 1992; Zik and Moses 1998). However, different from the microgravity opposed flame spread, the overall downward flame spread in normal gravity is stronger and more uniform than the microgravity flame spread in Fig. 3, so the flame can burn out the entire fuel.

There are two reasons for the stronger opposed flame spread in normal gravity. Firstly, when the flame is locally extinguished, the hot PE film can continue to curl and move downward (i.e., like a dripping flow), driven by both surface tension and gravity, to sustain a continuous flame leading edge. Secondly, the flame in the normal gravity is stronger due to a sufficient oxygen supply induced by the buoyancy. The flame is orange-color, bright, and strong (i.e., more soot particles formed), so that the flame radiant heating is much greater than the weak and blue flame in microgravity. In

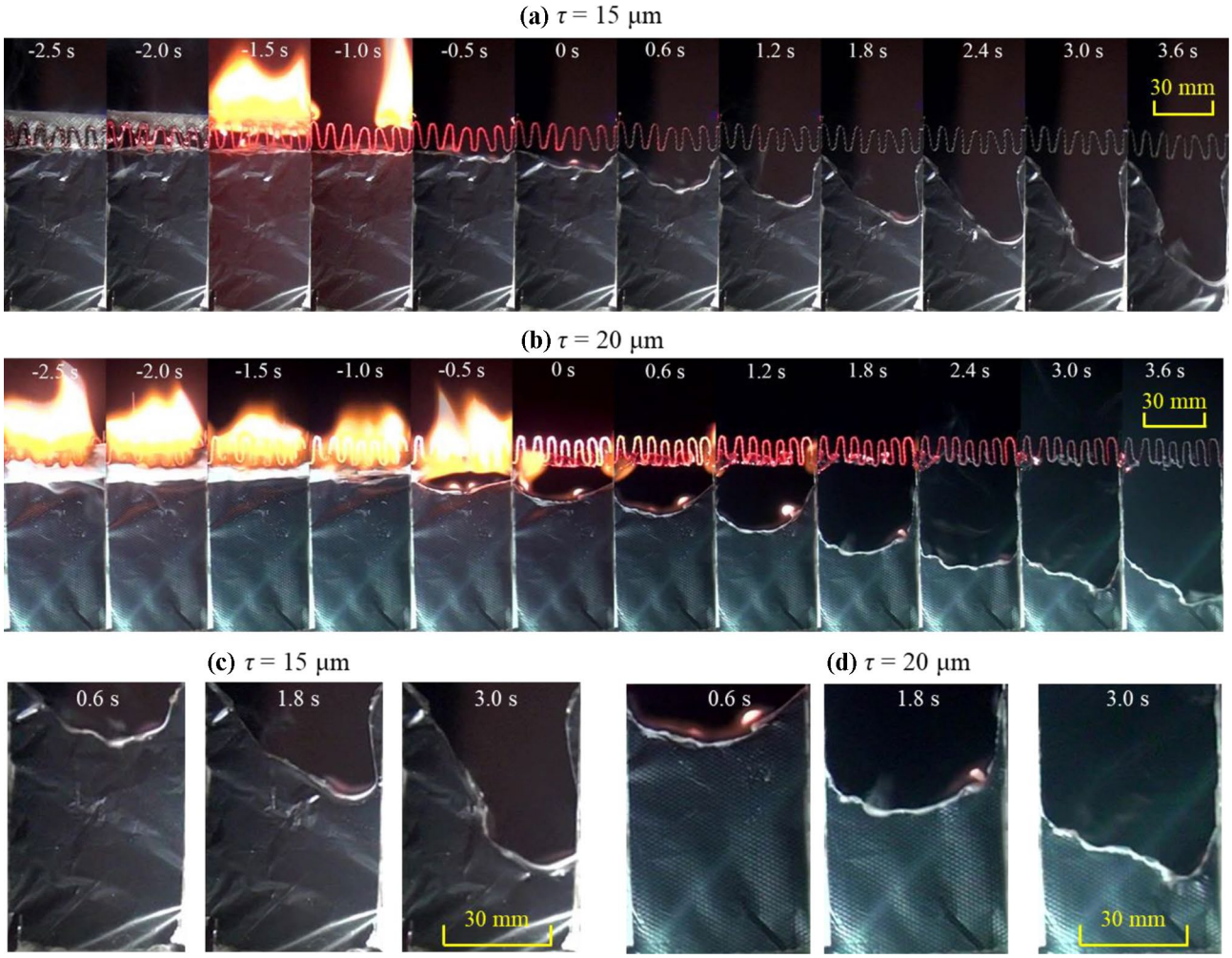

Fig. 3 Images of the flame spread process under microgravity environment, (**a**) 15-μm PE film, and (**b**) 20-μm PE film; Extinction process (**c**) 15-μm PE film, and (**d**) 20-μm PE film. (also see Videos S1 and S2)

short, both the dripping of molten PE and the strong flame heating are responsible for maintaining such a more robust downward flame spread.

Opposed Flame Spread Rate

For a spreading flame, the leading edge refers to the position where the flame travels with the fastest velocity, and a local spread rate V_f is represented by the traveling speed of the flame leading edge, and the raw data for the time history of the flame position are shown in Fig. 12. The spread rates of vertically downward flames determined in this way for the samples with different thicknesses are shown in Fig. 5a. The schematic diagram of the flame spread over PE film in the buoyancy-free microgravity, and buoyancy-driven normal gravity is shown in Fig. 5b. For the PE film used here, the temperature profile across the thickness is assumed to be uniform, as Biot number $Bi = h\tau/\lambda_s \approx 6 \times 10^{-4} \ll 0.1$, where λ_s is the thermal conductivity of the PE film, and the detailed calculation is provided in Appendix. It is evident that the flame spread rate tends to decrease with increasing thickness, and such a trend is in accordance with the theoretical prediction for thermally thin solid fuels (Quintiere 2006). What is interesting is that the flame spreads under a microgravity environment is clearly faster than the downward flame spread in a normal gravity environment.

There could be two factors that contribute to a larger flame spread in microgravity. Firstly, in the microgravity environment, dripping is absent, the molten fuel tends to accumulate driven by the surface tension to increase the burning rate and flame length. Secondly, without the upward buoyancy flow, the diffusion-controlled flame expands to increase the pre-heating intensity ($\dot{q}''_f = \dot{q}''_{con}$), and the degree of expansion increases with the size of molten fuel. Nevertheless, such a trend is the opposite to

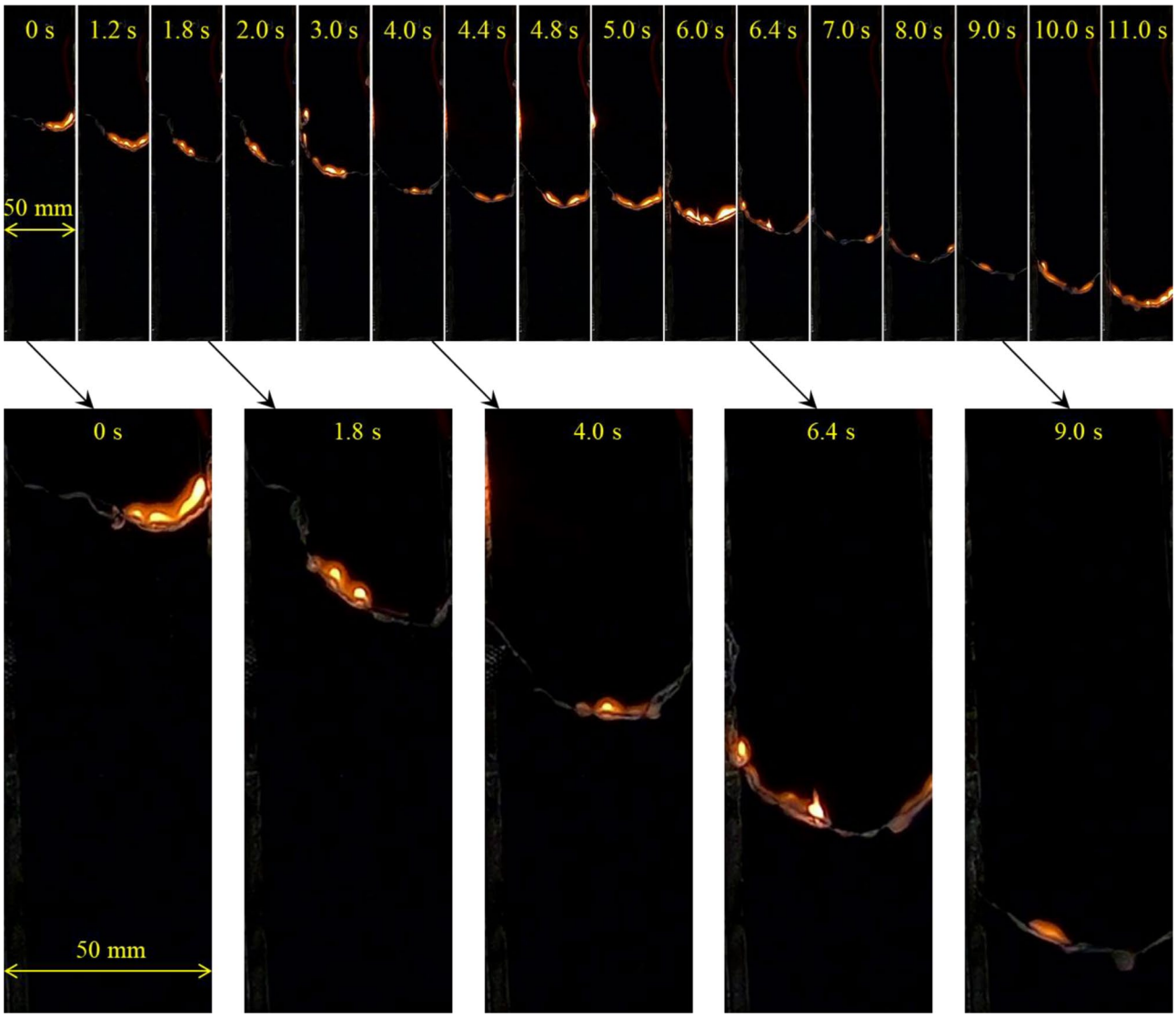

Fig. 4 Images of vertically downward flame spreading process under normal gravity ($\tau = 20$ μm)

the thin tissue papers. Olson et al. (Olson et al. 1989) showed that in the microgravity quiescent air environment, the flame spread rate is 0.54 cm/s, while in normal gravity natural convective environment, the downward flame spread rate is about 1.12 cm/s. The molten of PE could be the major reason for the difference from the thin tissue paper, but more research are need to further clarify.

For a downward spreading flame, it is driven by the heat transfer in the region ahead of a flame, i.e., the preheat zone. According to a simplified flame spread model illustrated in Fig. 5b, the preheat zone involves the flame heat flux ($\dot{q}_f''$) and the heat loss from the surface to the environment ($\dot{q}_\infty''$). Thus, the thermal-driven flame spread rate for a thermally thin fuel can be expressed as

$$V_f = \frac{\left(\dot{q}_f'' - \dot{q}_\infty''\right)\delta_f}{\rho_s c_s \tau \left(T_{ig} - T_\infty\right)} \tag{1}$$

where ρ_s, c_s, and τ are the density, specific heat, and thickness of the solid fuel; T_{ig} and T_∞ are the ignition temperature and ambient temperature. Therefore, regardless of the gravity level, the flame spread rate decreases as the thickness increases and eventually approaches a minimum at the thermally thick limit.

The flame preheating length (δ_f) can be estimated as

$$\delta_f = \frac{\alpha_g}{V_g} \tag{2}$$

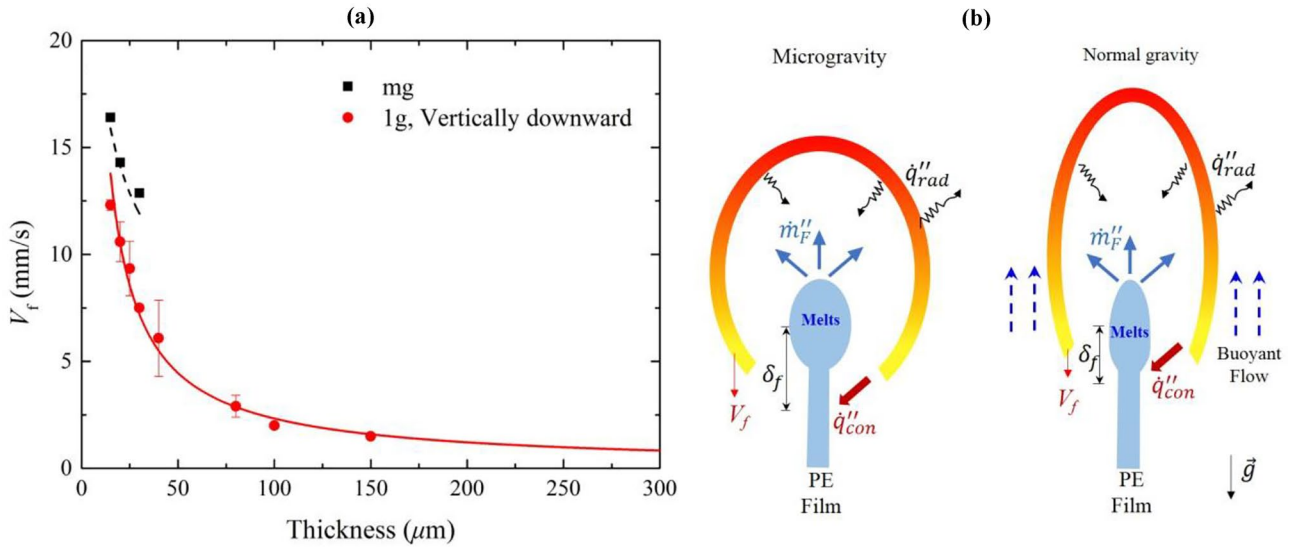

Fig. 5 (**a**) Variation of the opposed flame spread rate with the sample thickness; and (**b**) schematic diagram of the opposed flame spread over PE film in microgravity and normal gravity (downward spread)

which decreases as the opposed airflow velocity (V_g) increases. In the microgravity environment, the disappearance of the opposed airflow increases the flame preheating length, leading to a microgravity flame spread rate larger than that in normal gravity, as found in Fig. 5.

Note that in the preheat zone, the thermoplastic material will first melt before pyrolysis and ignition, different from thermoset materials like the cast PMMA. Once the thermoplastic in the preheat zone is melt, it will flow like a viscous liquid under the gravity and surface tension forces. Therefore, the melting flow can significantly increase the downward flame spread rate, as observed for the thick PMMA rod (Wu et al. 2020a) and PE wire (Kobayashi et al. 2018), and the observed global motion of flame also includes the flow of melts (V_m) as

$$V_{tot} = V_f + V_m \tag{3}$$

The flow velocity of melts can be estimated based on the balance between the driven force of gravity and (Marangoni) surface tension and the resistance of viscous force as

$$m_m g \sin\theta + \sigma_m l_m = \mu_m l_m V_m \tag{4}$$

$$V_m = \frac{m_m g \sin\theta + \sigma_m l_m}{\mu_m l_m} \propto l_m^2 \propto \tau^2 \tag{5}$$

where θ is the inclination angle of film sample, so $\theta = -90°$ and $\sin\theta = -1$ for the vertically downward spread; σ_m and μ_m are the surface tension, and viscosity of melts, respectively. The characteristic length of melts is proportional to the fuel thickness ($l_m \propto \tau$), so that the mass of melt also increases with the thickness ($m_m \propto l_m^3 \propto \tau^3$). For the ultra-thin PE film, the molten PE in the preheat zone is also small, and no dripping flow is observed. Thus, the influence of melting flow is negligible ($V_m \ll V_f$). On the other hand, as the fuel sample becomes thicker, and the preheating length of flame becomes larger, the melting flow will become important, and the dripping phenomenon will also occur in normal gravity.

Effect of Fuel Inclination and Gravity

To identify the normal-gravity fire scenarios that (1) have the largest fire hazard and (2) are closest to the microgravity condition, more normal-gravity flame-spread experiments are conducted for PE films of different inclinations. Representative flame images for downward ($\theta < 0$) and upward ($\theta < 0$) flame spread are shown in Fig. 6. The measured flame spread rates under different film inclinations are summarized in Fig. 7a.

For the downward flame spread, the flame leading edge is almost continuous and uniform, and the luminosity of the flame increases, as the fuel tilted from the vertical position. As the flame is anchored on the molten film, the flame length is almost the same for all the angles. When -90° ≤ θ ≤ -60°, the molten PE adheres to the unburned fuel sample, and no dripping flow can be observed. Therefore, it also supports that the influence of the gravity force and the melting flow on downward flame spread over ultra-thin film is negligible ($V_m \ll V_f$). As a result, a near-constant opposed flame spread rate is observed in this inclination region (see Fig. 7a).

With the increase of the inclination angle from -60° to 0° (horizontal), the opposed flame spread rate increases significantly (see Fig. 7a). By deviating the sample from the vertical downward, the preheating or contact length

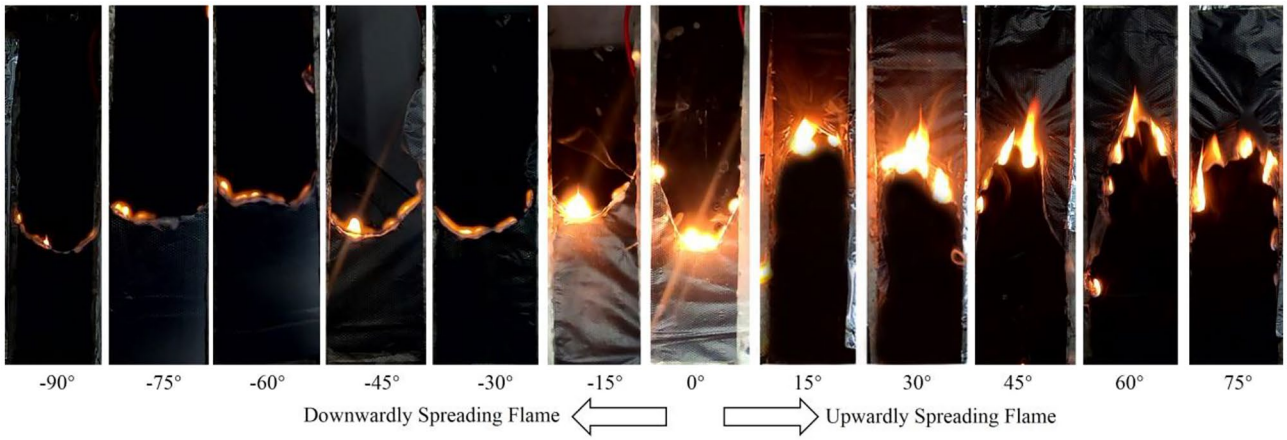

Fig. 6 Flame appearance under different angles ($\tau = 20$ μm)

between flame and fuel sample increases, so does the effective flame heat flux. A similar trend was also found for the flame spread over 0.16-mm card by Hirano et al. (Hirano et al. 1974). It is noted that the flame spread rate in the buoyancy-free microgravity is equal to that at $\theta =$ -45°, implying that the same contact of the flame with the unburned fuel sample.

Moreover, for $\theta \geq$ -45°, the dripping of molten PE starts to occur during the flame spreading process, and the dripping frequency also increases with the inclination. Such a phenomenon also indicates a stronger flame heating that can melt more fuel, exceeding the flame burning rate. Nevertheless, because most melting fuels are dripped to the ground rather than flow on the fuel sample, the influence of melting and dripping on the opposed downward flame spread over thin PE film is still relatively small.

For upward spreading flame over thin wires with PE insulation, the rate of concurrent flame can reach steady-state (Hu et al. 2015; Lu et al. 2019b), despite potential downward dripping flows (Nagachi et al. 2019). In this study, the upward spreading flame on thinner PE film also reaches a semi-steady state. The flame spread rate increases with the inclination when the angle is less than 30°. When the inclination angle is larger than 30°, the upward flame spread rate is almost constant along the fuel surface, and a maximum spread rate is reached (see Fig. 7a). The maximum rate is about 45 ± 10 mm/s for the 20-mm PE film. It is mainly because the dripping removal (detachment) of molten PE that prevents the further growth of burning zone and flame length.

Note that such a trend of upward flame spread rate on PE film is different from thin papers (see comparison in

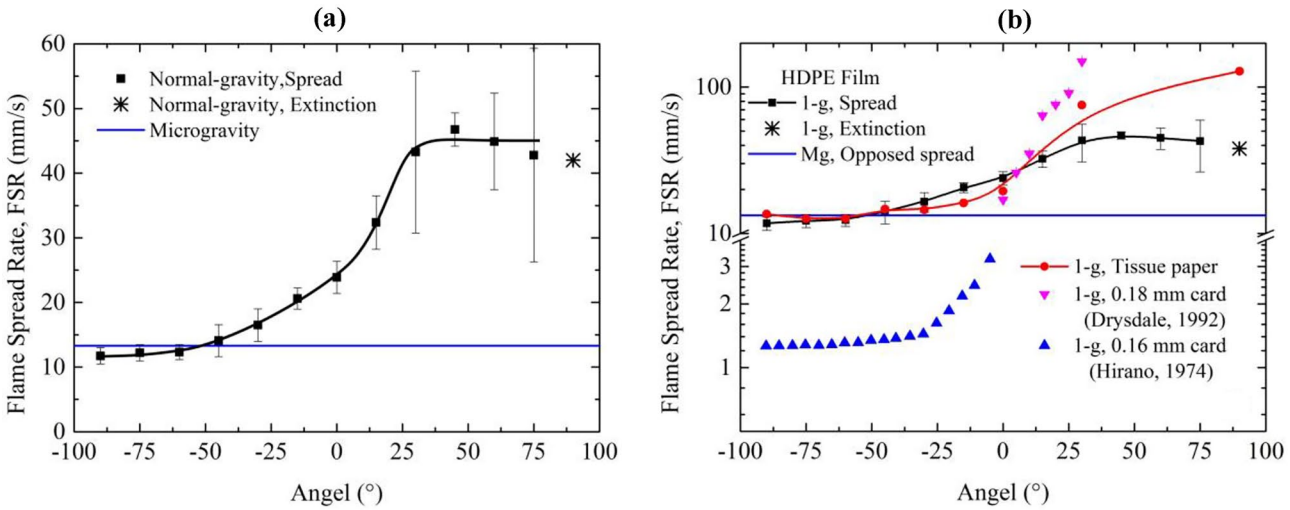

Fig. 7 Variation of flame spread rate with fuel inclination angles and the extinction limit, (**a**) normal coordinate and (**b**) logarithm coordinate, where the film thickness is $\tau = 20$ μm

Fig. 7b) and thin wires. In fact, for all other thin fuels, the upward flame spread rate monotonically increases with the increased angle (Hirano et al. 1974; Hu et al. 2015; Lu et al. 2019b) and reaches the maximum at 90° (i.e., the vertical upward). For flame spread over thin PE-insulated wires, although the melt droplet sliding along the metal core, dripping is detached from the wire. Thus, the melt fuel still increases the burning zone and flame length in wire, accelerating the flame spread.

The average fuel melting rate ($\dot{m}_m$), burning rate ($\dot{m}_b$), and dripping rate ($\dot{m}_{dr}$) are also quantified for different fuel inclination angles based on the mass conservation.

$$\dot{m}_m = \dot{m}_b + \dot{m}_{dr} \tag{6}$$

The melting rate is calculated by the linear fitting of the mass-loss curve; the average dripping rate is calculated by the landed dripping mass; and then, the burning rate can be estimated. All three mass-loss rates are summarized in Fig. 8a and compared with the upward flame-spread rate. Note that there is a clear similarity in the shape of curve between the burning rate and the flame spread rate. As the inclination approaches to the vertical upward, a larger portion of molten fuel is dripped.

For upward flame spread, the flame spread rate is controlled primarily by the flame heat flux to the unburnt fuel upward (Loh and Fernandez-Pello 1985). For a small flame (< 5 cm) in this work, and the convective heating by the flame contact is dominant over the radiation (Orloff et al. 1975). As a first approximation, the flame convective heat flux ($\dot{q}_f''$) is proportional to the natural convection coefficient ($h = \lambda_g Nu/L$) as

$$\dot{q}_f'' \propto h \propto Nu \propto Ra^{\frac{1}{4}} \propto (sin\theta)^{\frac{1}{4}} \tag{7}$$

where λ_g, L, Nu, and Ra are gas thermal conductivity, flame length, Nusselt number, and Rayleigh number, respectively. Thus, the flame heat flux increases with the increased inclination angle, resulting in an increased melting rate, agreeing with Fig. 8a.

The fast melting process during the flame spread also increase the rate of dripping. There is an upper size limit of the molten ball (D),

$$M_{dr}g = \frac{\pi}{6}\rho_m D^3 g \geq \sigma_m l_m \tag{8}$$

above which its gravity will overcome its surface tension force ($\sigma_m l_m$), resulting in the dripping process (Kobayashi et al. 2017). The critical diameter of the PE droplet at the moment of detachment was measured, and the maximum diameter and the average diameter were shown in Fig. 8b (see detailed dripping process in Video S5). Here, the average diameter is defined as the average of all the droplet diameters during the dripping process. Clearly, the critical diameter is almost the same for all the angles, agreeing with Eq. (8), and the molten ball drops when it reaches a critical mass.

In summary, there are two competing mechanisms that control the upward flame spread rate, (I) the flame convective heat flux ($\dot{q}_f'$), and (II) the burning rate or the flame size. As the inclination angle increases and approaches to vertical upward (90°), the flame heat flux increases, as shown in Eq. (7), and the total melting rate increases, as shown in Fig. 8. As the inclination angle is less than 30°, the melting rate

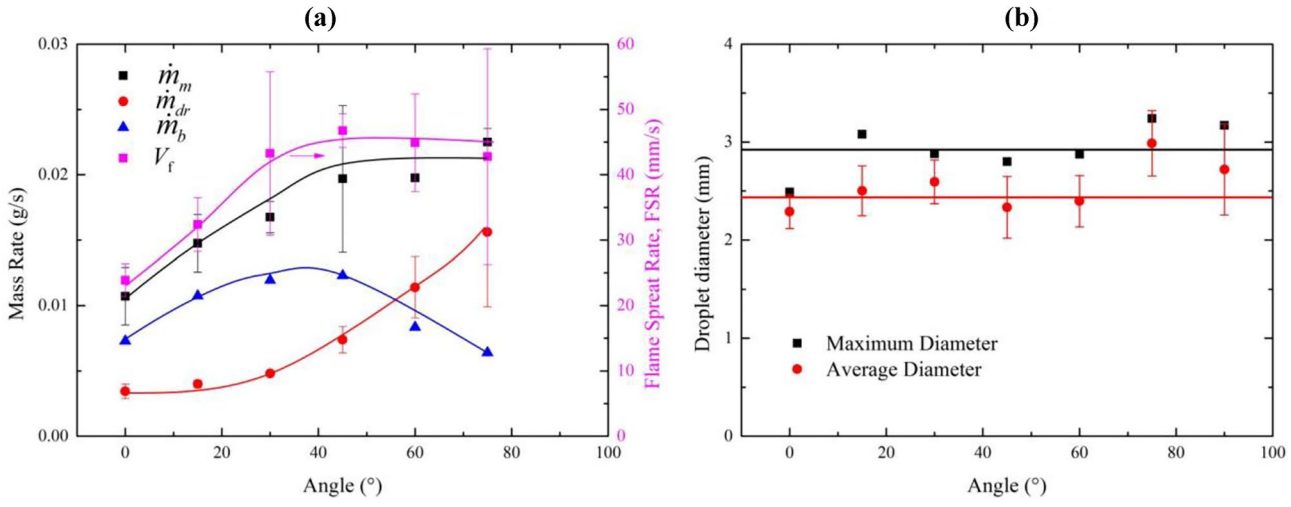

Fig. 8 Variation of mass loss rate (**a**) and droplet diameter (**b**) with fuel inclination angles for upward spread flame

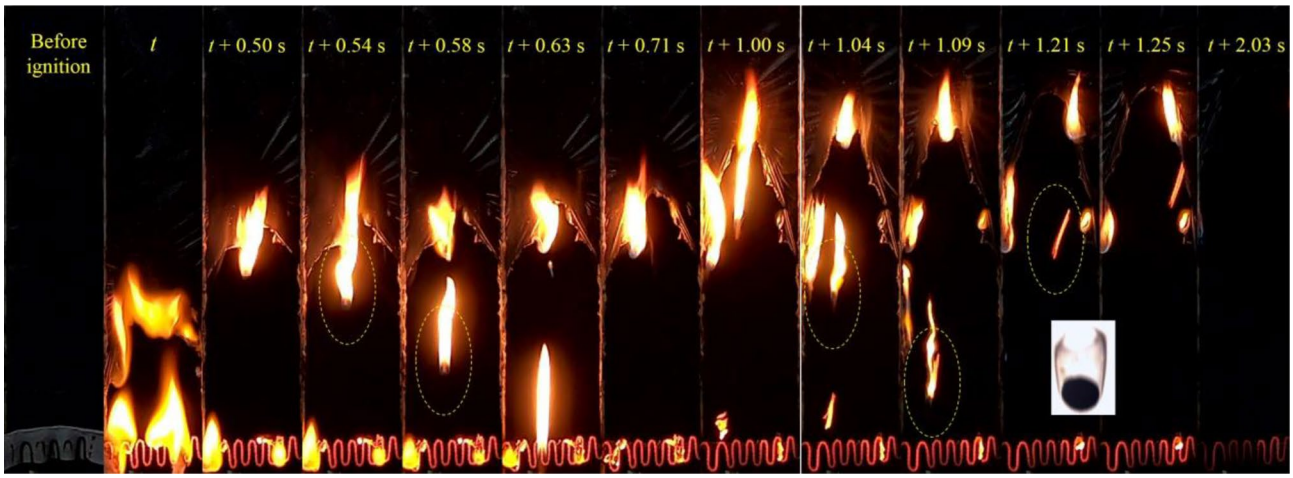

Fig. 9 A typical dripping and extinction process of upward flame spread ($\theta = 90°$) with the 20-μm thin PE film (see Video S4)

increases faster than the dripping rate, resulting in the increasing burning rate. Then, flame length (δ_f in Eq. (1)) increases the flame heating and the flame spread rate. As the inclination angle is above 30°, the burning rate becomes large for all the angles and flame length becomes almost the same, resulting in a maximum flame spread rate. Therefore, the overall upward flame spread rate changes under the competition between the enhanced flame heating by the buoyancy and the reduced flame size by the dripping removal of the molten fuel.

Self-extinction in Normal Gravity by Dripping

With the increase of the inclination angle, the contacting flame area with the unburned film is increased, resulting in the increase of the molten PE and the rate of its evaporation, thus, increasing the flame spread rate. However, as the PE sample is upwardly placed, the molten PE drips and removes the fuel, resulting in a reduced flame spread rate. When the inclination angle is 90°, the fuel is removed, resulting in flame extinction. The extinction process for the film with a thickness of 20 μm is shown in Fig. 9 (see Video S4). It is clear that after the ignition of the sample, large PE molten droplet drips to the ground. After about 2 s, the flame extinguishes. When the film thickness is in the range of 15–40 μm, the vertically upwardly spreading flames all extinguish. This flame spread behavior is significantly different from the thermosetting plastics that have no dripping tendency. The schematic diagram of the flame spread over PE film is shown in Fig. 10. For an upwardly spreading flame, the molten PE droplet is tilted by the buoyant flow. Once the droplet

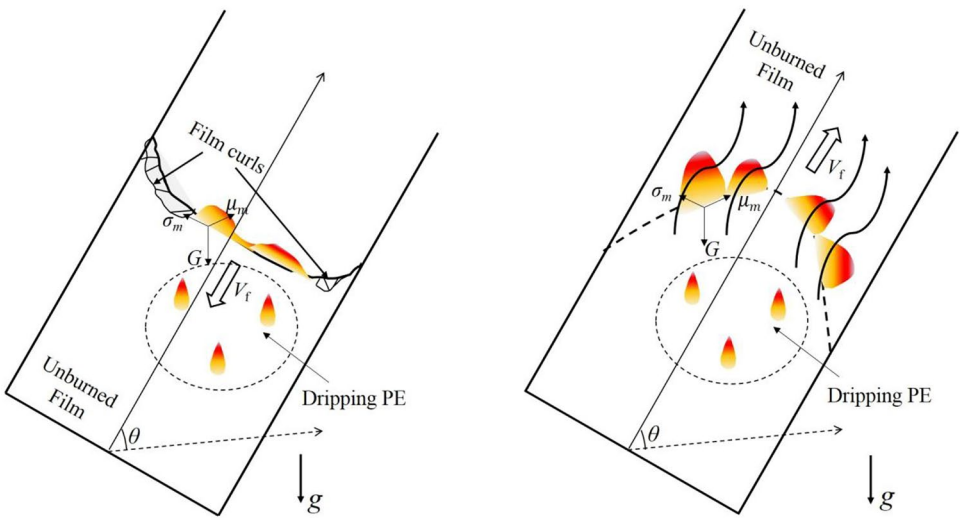

(a) Downward flame spread **(b)** Upward flame spread

Fig. 10 Schematic diagram of the flame spread over PE film with different fuel inclinations, (**a**) downward flame spread and (**b**) upward flame spread

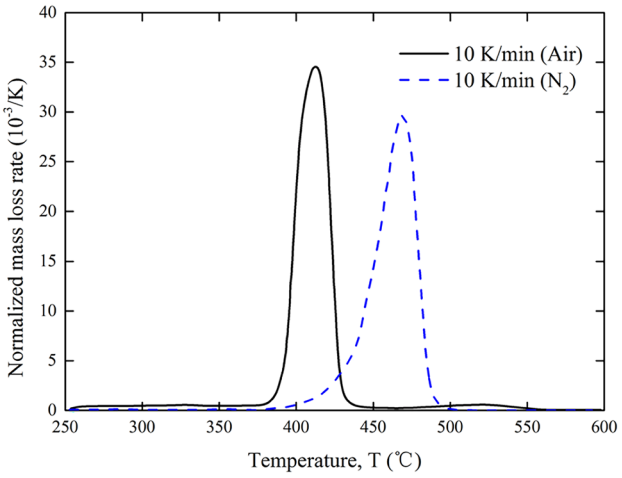

Fig. 11 DTG curves of HDPE at the heating rate of 10 K/min

detached from the unburned film, the dripping tail often breaks into small drips. For vertically upwardly spreading flame, the molten PE is accumulated into one large droplet, as is shown in Fig. 9 and Video S5.

Conclusions

This work investigates the flame spread of diffusion flames along 15–100 μm thin polyethylene (PE) film in both drop-tower microgravity and normal gravity environments. The revealed influence of gravity and angular orientation on the flame-spread behavior are summarized as follows:

(1) In microgravity, the uniform flame leading edge cannot be sustained on PE films, and the flame spreads with partial and local extinction. However, in normal gravity, although the local extinction occurs during flame spreading vertically downwardly, the leading edge can be sustained uniform with partial unburned curling edges rolling down. Microgravity flame spread faster than vertically downward flame spread in normal gravity due to the weak buoyancy flow and greater flame preheating length. For thin films, the influence of melting on the opposed flame spread is negligible.

(2) The downward flame spread displays a slight increase when the orientation angle is in the range of -90° to -45° measured with respect to the horizontal (0°). With the increase of the inclination angle, the flame spread rate has a greater increase. The upward flame spread first increases and then reaches a constant maximum when the angle is larger than 30°. The maximum flame spread rate for a 20-μm thickness PE film is 45 ± 10 mm/s.

(3) For vertically upward fire spreading, the flame cannot be survived after a short spreading due to the dripping effects of the molten material on the removal of the combustible material. This flame-spread experiment on the thin PE films could provide valuable data and guidelines for more sophisticated fire safety tests for space travel.

Appendix

The thermogravimetric analysis (TGA) analysis of PE sample was conducted with a PerkinElmer STA 6000 Simultaneous Thermal Analyser. The initial mass of PE sample was 3–5 mg, and samples were heated at the constant rate of 10 K/min and under both nitrogen and air environments. Experiments were repeated twice for each case, and good repeatability is shown. Figure 11 shows the mass-loss rate

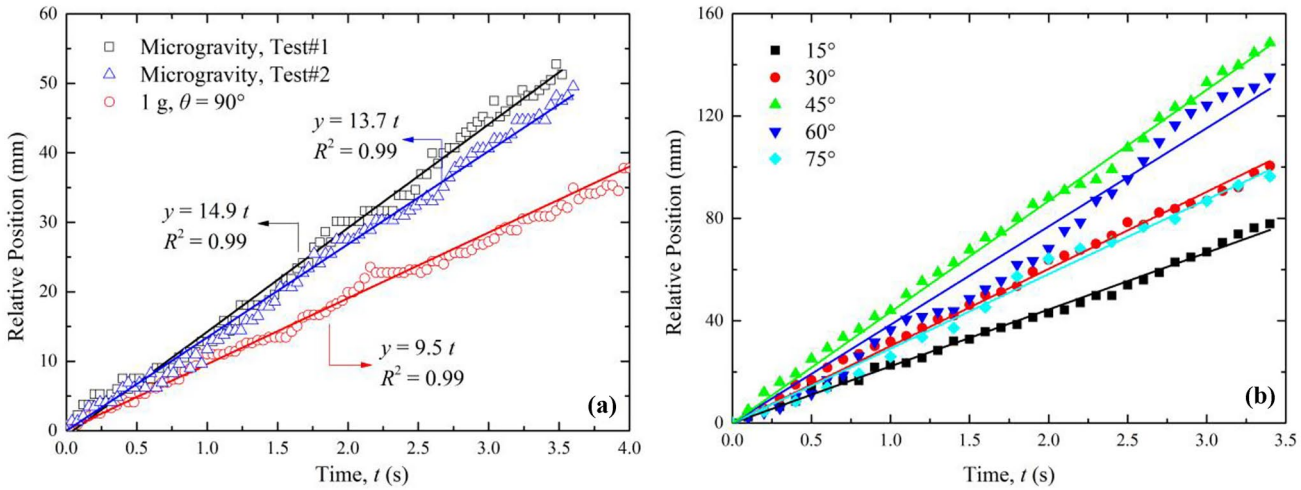

Fig. 12 The time evolution of the flame leading edge position for the film with a thickness of 20 μm for (**a**) downward flame spread and microgravity flame spread (**b**) upward flame spread

Table 1 Properties of air at 450 K (Incropera et al. 2013)

Parameters	Parameter values	Units
λ_g	0.0643	W/(m K)
ν	112.2×10^{-6}	m^2/s
α	155×10^{-6}	m^2/s
Pr	0.723	-
β	0.001	K^{-1}

curves of the PE insulation sample. In general, the pyrolysis temperature of PE is about 410 °C, and the ignition temperature is slightly higher.

The position of flame leading edge as a function of time under microgravity experiments and normal gravity environment for the vertically downward spreading flame. The coefficients of determination (R^2) for each fitting curve are listed in the Fig. 12.

The Bi number is defined as $Bi = h\tau/\lambda_s$, where h is the heat-transfer coefficient, τ is the thickness of the film, which is used as the characteristic length, λ_s is the thermal conductivity of the film. We first determine the flow condition and the heat transfer coefficient.

$$Ra_L = \frac{g\beta\left(T_{ig} - T_\infty\right)L^3}{\alpha\nu} = 1 \times 10^6 \ll 10^9$$

Thus, the flow is laminar, and we can estimate the convection coefficient as

$$\bar{N}u_L = 0.68 + \frac{0.670Ra_L^{1/4}}{\left[1 + (0.492/\mathrm{Pr})^{9/16}\right]^{4/9}}$$

$$h = \frac{\bar{N}u_L\lambda_g}{L} = 7.4\ \mathrm{W/m^2K}$$

Then, the Bi number can be calculated for PE film of $\tau = 40$ μm as

$$Bi = \frac{h\tau}{\lambda_s} = 6 \times 10^{-4}$$

where properties of gas are evaluated at the film temperature $T_f = \left(T_{ig} + T_f\right)/2 = 950K$, where T_{ig} is the ignition temperature of the PE, and T_f is the flame temperature. The properties of air are shown in Table 1. The length of the sample is used as the characteristic length, that is $L = 0.15$ m.

Supplementary Information The online version contains supplementary material available at https://doi.org/10.1007/s12217-022-09945-4.

Funding This work is supported by the National Key R&D Program of China (Grant No. 2021YFA0716203), the Opening Fund of State Key Laboratory of Fire Science (SKLFS) under Grant No. HZ2021-KF12, and the National Natural Science Foundation of China under Grant No. U1738117.

Declarations

Conflict of Interest None.

References

Altenkirch, R.A., Tang, L., Sacksteder, K., Bhattacharjee, S., Delichatsios, M.A.: Inherently unsteady flame spread to extinction over thick fuels in microgravity. Symp. Int. Combust. **27**(2), 2515–2524 (1998)

Bhattacharjee, S., Ayala, R., Wakai, K., Takahashi, S.: Opposed-flow flame spread in microgravity-theoretical prediction of spread rate and flammability map. Proc. Combust. Inst. **30**, 2279–2286 (2005). https://doi.org/10.1016/j.proci.2004.08.020

Bhattacharjee, S., Wakai, K., Takahashi, S.: Predictions of a critical fuel thickness for flame extinction in a quiescent microgravity environment. Combust. Flame. **132**, 523–532 (2003). https://doi.org/10.1016/S0010-2180(02)00501-1

Comas, B., Pujol, T.: Flame front speed and onset of instability in the burning of inclined thin solid fuel samples. Phys. Rev. E Stat. Nonlinear. Soft. Matter. Phys. **88**, 12–17 (2013). https://doi.org/10.1103/PhysRevE.88.063019

Drysdale, D.D., Macmillan, A.J.R.: Flame spread on inclined surfaces. Fire. Saf. J. **18**, 245–254 (1992). https://doi.org/10.1016/0379-7112(92)90018-8

Fernandez-Pello, A.C., Ray, S.R., Glassman, I.: Flame spread in an opposed forced flow: the effect of ambient oxygen concentration. Symp. Int. Combust. **18**, 579–589 (1981). https://doi.org/10.1016/S0082-0784(81)80063-X

Fujita, O.: Solid combustion research in microgravity as a basis of fire safety in space. Proc. Combust. Inst. **35**, 2487–2502 (2015). https://doi.org/10.1016/j.proci.2014.08.010

Fujita, O., Nishizawa, K., Ito, K.: Effect of low external flow on flame spread over polyethylene-insulated wire in microgravity. Proc. Combust. Inst. **29**, 2545–2552 (2002). https://doi.org/10.1016/s1540-7489(02)80310-8

Gollner, M.J., Huang, X., Cobian, J., Rangwala, A.S., Williams, F.A.: Experimental study of upward flame spread of an inclined fuel surface. Proc. Combust. Inst. **34**, 2531–2538 (2013). https://doi.org/10.1016/j.proci.2012.06.063

Hirano, T., Noreikis, S.E., Waterman, T.E.: Postulations of flame spread mechanisms. Combust. Flame. **22**, 353–363 (1974). https://doi.org/10.1016/0010-2180(74)90050-9

Hu, L., Zhang, Y., Yoshioka, K., Izumo, H., Fujita, O.: Flame spread over electric wire with high thermal conductivity metal core at different inclinations. Proc. Combust. Inst. **35**, 2607–2614 (2015). https://doi.org/10.1016/j.proci.2014.05.059

Hu, W.R., Zhao, J.F., Long, M., Zhang, X.W., Liu, Q.S., Hou, M.Y., Kang, Q., Wang, Y.R., Xu, S.H., Kong, W.J., Zhang, H., Wang, S.F., Sun, Y.Q., Hang, H.Y., Huang, Y.P., Cai, W.M., Zhao, Y., Dai, J.W., Zheng, H.Q., Duan, E.K., Wang, J.F.: Space program {SJ}-10 of microgravity research. Microgravity. Sci. Technol. **26**, 159–169 (2014)

Ikeda, M.: Effects of gravity on ignition and combustion characteristics of externally heated polyethylene film. Microgravity. Sci. Technol. **30**, 331–338 (2018). https://doi.org/10.1007/s12217-018-9606-9

Incropera, F., Lavine, A., Bergman, T., DeWitt, D.: Principles of heat and mass transfer. Wiley (2013)

Ito, A., Kashiwagi, T.: Characterization of flame spread over PMMA using holographic interferometry sample orientation effects.

Combust. Flame. **71**, 189–204 (1988). https://doi.org/10.1016/0010-2180(88)90007-7
Kobayashi, Y., Huang, X., Nakaya, S., Tsue, M., Fernandez-Pello, C.: Flame spread over horizontal and vertical wires: The role of dripping and core. Fire. Saf. J. **91**, 112–122 (2017). https://doi.org/10.1016/j.firesaf.2017.03.047
Kobayashi, Y., Konno, Y., Huang, X., Nakaya, S., Tsue, M., Hashimoto, N., Fujita, O., Fernandez-Pello, C.: Effect of insulation melting and dripping on opposed flame spread over laboratory simulated electrical wires. Fire. Saf. J. **95**, 1–10 (2018). https://doi.org/10.1016/j.firesaf.2017.10.006
Kobayashi, Y., Terashima, K., bin Borhan, M.A.F., Takahashi, S.: Opposed flame spread over polyethylene under variable flow velocity and oxygen concentration in microgravity. Fire. Technol. **56**, 113–130 (2020). https://doi.org/10.1007/s10694-019-00862-4
Kumar, A., Shih, H.Y., T'ien, J.S.: A comparison of extinction limits and spreading rates in opposed and concurrent spreading flames over thin solids. Combust. Flame. 132, 667–677 (2003). https://doi.org/10.1016/S0010-2180(02)00516-3
Link, S., Huang, X., Fernandez-Pello, C., Olson, S., Ferkul, P.: The Effect of Gravity on Flame Spread over PMMA Cylinders. Sci. Rep. **8**, 120 (2018). https://doi.org/10.1038/s41598-017-18398-4
Loh, H.T., Fernandez-Pello, A.C.: A study of the controlling mechanisms of flow assisted flame spread. Symp. Int. Combust. **20**, 1575–1582 (1985). https://doi.org/10.1016/S0082-0784(85)80652-4
Lu, Y., Huang, X., Hu, L., Fernandez-Pello, C.: Concurrent flame spread and blow-off over horizontal thin electrical wires. Fire. Technol. **55**, 193–209 (2019a). https://doi.org/10.1007/s10694-018-0785-0
Lu, Y., Huang, X., Hu, L., Fernandez-Pello, C.: The interaction between fuel inclination and horizontal wind: Experimental study using thin wire. Proc. Combust. Inst. **37**, 3809–3816 (2019b). https://doi.org/10.1016/j.proci.2018.05.131
Migita, T., Yamahata, T., Strempfl, P., Matsuoka, T., Nakamura, Y.: Methodology to Achieve Pseudo 1-D Combustion System of Polymeric Materials Using Low-Pressured Technique. Fire. Technol. **56**, 229–245 (2020). https://doi.org/10.1007/s10694-019-00877-x
Miyamoto, K., Huang, X., Hashimoto, N., Fujita, O., Fernandez-Pello, C.: Limiting oxygen concentration (LOC) of burning polyethylene insulated wires under external radiation. Fire. Saf. J. **86**, 32–40 (2016). https://doi.org/10.1016/j.firesaf.2016.09.004
Nagachi, M., Mitsui, F., Citerne, J.M., Dutilleul, H., Guibaud, A., Jomaas, G., Legros, G., Hashimoto, N., Fujita, O.: Can a spreading flame over electric wire insulation in concurrent flow achieve steady propagation in microgravity? Proc. Combust. Inst. **37**, 4155–4162 (2019). https://doi.org/10.1016/j.proci.2018.05.007
NASA-STD-6001B: Flammability, offgassing, and compatibility requirements and test procedures. Test 1, Upward Flame Propagation. (2011)
Olson, S.L.: Mechanisms of Microgravity Flame Spread Over a Thin Solid Fuel: Oxygen and Opposed Flow Effects. Combust. Sci. Technol. **76**, 233–249 (1991). https://doi.org/10.1080/00102209108951711
Olson, S.L., Baum, H.R., Kashiwagi, T.: Finger-like smoldering over thin cellulosic sheets in microgravity. Symp. Int. Combust. **27**, 2525–2533 (1998)
Olson, S.L., Ferkul, P. V., T'ien, J.S.: Near-limit flame spread over a thin solid fuel in microgravity. Symp. Int. Combust. **22**, 1213–1222 (1989). https://doi.org/10.1016/S0082-0784(89)80132-8
Olson, S.L., Hegde, U., Bhattacharjee, S., Deering, J.L., Tang, L., Altenkirch, R.A.: Sounding rocket microgravity experiments elucidating diffusive and radiative transport effects on flame spread over thermally thick solids. Combust. Sci. Technol. **176**, 557–584 (2004)
Orloff, L., De Ris, J., Markstein, G.H.: Upward turbulent fire spread and burning of fuel surface. Symp. Int. Combust. **15**, 183–192 (1975). https://doi.org/10.1016/S0082-0784(75)80296-7
Quintiere, J.G.: The effects of angular orientation on flame spread over thin materials. Fire. Saf. J. **36**, 291–312 (2001). https://doi.org/10.1016/S0379-7112(00)00051-5
Quintiere, J.G.: Fundamentals of fire phenomena. John Wiley (2006)
Ramachandra, P.A., Altenkirch, R.A., Bhattacharjee, S., Tang, L., Sacksteder, K., Katherine Wolverton, M.: The behavior of flames spreading over thin solids in microgravity. Combust. Flame. **100**, 71–84 (1995). https://doi.org/10.1016/0010-2180(94)00046-U
Rojas-Alva, U., Jomaas, G.: A historical overview of experimental solid combustion research in microgravity. Acta. Astronaut. (2022). https://doi.org/10.1016/j.actaastro.2022.01.037
Rojas-Alva, U., Møller-Poulsen, F., Man, S.L., Creamer, C., Hanna, D., Jomaas, G.: Flame spread behaviour of Polydimethylsiloxane (PDMS) membranes in 1 g and μg environments. Combust. Flame. **240** (2022). https://doi.org/10.1016/j.combustflame.2022.112009
Ross, H.D.: Microgravity combustion: Fire in Free Fall. Academic Press (2001)
Sun, P., Wu, C., Zhu, F., Wang, S., Huang, X.: Microgravity combustion of polyethylene droplet in drop tower. Combust. Flame **222**, 18–26 (2020). https://doi.org/10.1016/j.combustflame.2020.08.032
Takahashi, S., Borhan, M.A.F. Bin, Terashima, K., Hosogai, A., Kobayashi, Y.: Flammability limit of thin flame retardant materials in microgravity environments. Proc. Combust. Inst. **37**, 4257–4265 (2019). https://doi.org/10.1016/j.proci.2018.06.102
Takahashi, S., Takeuchi, H., Ito, H., Nakamura, Y., Fujita, O.: Study on unsteady molten insulation volume change during flame spreading over wire insulation in microgravity. Proc. Combust. Inst. **34**, 2657–2664 (2013). https://doi.org/10.1016/j.proci.2012.06.158
Takahashi, S., Terashima, K., bin Borhan, M.A.F., Kobayashi, Y.: Relationship between blow-Off behavior and limiting oxygen concentration in microgravity environments of flame retardant materials. Fire. Technol. **56**, 169–183 (2020). https://doi.org/10.1007/s10694-019-00880-2
Tewarson, A.: Flammability of Polymers. John Wiley & Sons, Inc (2003)
Urban, D.L., Ferkul, P., Olson, S., Ruff, G.A., Easton, J., T'ien, J.S., Liao, Y.T., Li, C., Fernandez-Pello, C., Torero, J.L., Legros, G., Eigenbrod, C., Smirnov, N., Fujita, O., Rouvreau, S., Toth, B., Jomaas, G.: Flame spread: Effects of microgravity and scale. Combust. Flame. **199**, 168–182 (2019). https://doi.org/10.1016/j.combustflame.2018.10.012
Vetturini, A., Cui, W., Liao, Y.T., Olson, S., Ferkul, P.: Flame Spread Over Ultra-thin Solids: Effect of Area Density and Concurrent-Opposed Spread Reversal Phenomenon. Fire. Technol. **56**, 91–111 (2020). https://doi.org/10.1007/s10694-019-00878-w
Wang, S., Hu, J., Xiao, Y., Ren, T., Zhu, F.: Opposed-flow Flame Spread Over Solid Fuels in Microgravity: the Effect of Confined Spaces. Microgravity. Sci. Technol. **27**, 329–336 (2015). https://doi.org/10.1007/s12217-015-9419-z
Wang, S., Zhu, F.: Flame Spread in Low-Speed Forced Flows: Ground- and Space-Based Experiments. In: Wenrui, H., Qi, K. (eds.) Physical Science Under Microgravity: Experiments on Board the SJ-10 Recoverable Satellite, pp. 237–262. Research for Development. Springer, Singapore (2019)
West, J., Tang, L., Altenkirch, R.A., Bhattacharjee, S., Sacksteder, K., Delichatsions, M.A.: Quiescent flame spread over thick fuels in microgravity. Symp. Int. Combust. **26**, 1335–1343 (1996). https://doi.org/10.1016/S0082-0784(96)80352-3
Wu, C., Huang, X., Wang, S., Zhu, F., Yin, Y.: Opposed Flame Spread over Cylindrical PMMA Under Oxygen-Enriched Microgravity

Environment. Fire. Technol. **56**, 71–89 (2020a). https://doi.org/10.1007/s10694-019-00896-8

Wu, C., Sun, P., Wang, X., Huang, X., Wang, S.: Flame Extinction of Spherical PMMA in Microgravity: Effect of Fuel Diameter and Conduction. Microgravity. Sci. Technol. **32**, 1065–1075 (2020b). https://doi.org/10.1007/s12217-020-09829-5

Zhang, Y., Ronney, P.D., Roegner, E.V., Greenberg, J.B.: Lewis number effects on flame spreading over thin solid fuels. Combust. Flame. **90**, 71–83 (1992). https://doi.org/10.1016/0010-2180(92)90136-D

Zhao, X., Liao, Y.T.T., Johnston, M.C., T'ien, J.S., Ferkul, P. V., Olson, S.L.: Concurrent flame growth, spread, and quenching over composite fabric samples in low speed purely forced flow in microgravity. Proc. Combust. Inst. **36**, 2971–2978 (2017). https://doi.org/10.1016/j.proci.2016.06.028

Zhou, Y., Bu, R., Yi, L., Sun, J.: Heat transfer mechanism of concurrent flame spread over rigid polyurethane foam: Effect of ambient pressure and inclined angle. Int. J. Therm. Sci. **155**, 106403 (2020). https://doi.org/10.1016/j.ijthermalsci.2020.106403

Zhu, F., Lu, Z., Wang, S., Yin, Y.: Microgravity diffusion flame spread over a thick solid in step-changed low-velocity opposed flows. Combust. Flame. **205**, 55–67 (2019). https://doi.org/10.1016/j.combustflame.2019.03.040

Zik, O., Moses, E.: Fingering instability in solid fuel combustion: The characteristic scales of the developed state. Symp. Int. Combust. **27**, 2815–2820 (1998). https://doi.org/10.1016/S0082-0784(98)80139-2